A NUMERICAL STUDY OF THE HYDRAULIC AND THERMAL PERFORMANCE OF MCHS CONTAINING NANOFLUIDS WITH POROUS SUBSTRATES

HUDA RIDHA

Veterinary Medicine College, Wasit University, Wasit , Iraq
E-mail: hridha@uowasit.edu.iq

Abstract - The use of microchannel heat sinks with porous media has been shown to reduce pressure drop and improve heat transfer. An optimization study is presented in this study that evaluates the impacts of porous thickness on the hydoplics and thermal performance of porous microchannel heat sinks (MCHS). Pressure drops increased with increased porous thickness. However, there is not an optimum pressure drop. Adding a porous structure improves heat transfer for fins in the thickness range studied in this paper. Heat transfer coefficients have been found to be exponentially related to solid thicknesses for all solid thicknesses. Moreover, when the fraction of nanofluid volume increases, so does the heat transfer coefficient and Reynolds number. A velocity of 1.2 m/s caused the greatest change in pressure drop and heat transfer coefficient with porous thickness. Variations of the parameters decrease with decreasing velocity.

Keywords - Microchannel, Heatsink, Porous, Heat transfer, Nanofluid, Optimization

I. INTRODUCTION

Cooling is a major concern in many industries, such as electronics, chemical steam tools, solar collectors, and many more[1-4]. In order to prevent mechanical devices from wearing out or permanently damage electronic equipment, temperatures must be lowered in order to prevent hot spots. Therefore, an efficient cooling system is essential to minimize the thermal load on the system and ensure maximum effectiveness in various conditions[2, 4-10]. A device or system may not work or, worse, may be damaged if too much heat cannot be dissipated rapidly.Therefore, heat transfer technologies with high efficiency are essential. One of the primary heat transfer problems in such applications is the limited equipment space.

Rapid developments in the computer industry have also posed considerableissues in terms of cooling methods for electronics.The performance of these devices is heavily affected by the cooling mechanisms behind them. In this case, microchannel heat sinks are suitable options. Microchannel heating wells are small heat exchangers that can transfer large amounts of heat from small surfaces. Since the first work by Tuckerman and Pease [11], many studies have been pefrormed to study the MCHS's thermal performance and hydraulic properties.A copper microchannel was constructed by Qu and Mudawar[8] and tested at varying heat fluxes. These researchers used a mathematical model to obtain pressure drop and temperature distribution, which was then corroborated with the traditional theory of ordinary channels.The use of geometrical factors for improving the cooling effectiveness of MCHS has been extensively studied including microchannel pattern, cross-section geometry, manifold, and inlets/outlets [12]. There has been research on changing geometric parameters to impact pressure drops, mean temperatures, and heat transfer coefficients. Kumar et al. 14, 15] reviewed works describing how inlet and outlet configurations influencehydraulic and thermal effectiveness. According to this study, the vertical supplies and collection systems are less non-uniform in temperature and better in fluid flow patterns. Wang et al. [13]introduced a two-layer wave MCHS featuring porous gears, and discovered that the porous gears showed a clear advantage in low pumping power. Li et al. [14]undertook a study comparing the flow behavior and thermal effectiveness of five different heat sinks,consisting of single-layer porous gears, single-layer gears, two-layer gears, two-layer porous gears, and two-layer mixtures. They reported that two-layer MCHS involves low pressure drops and have high thermal efficiency.

To the best of our knowledge, the flow of nanofluids in porous-MCHSs is not widely studied. Studies from Bezaatpour and Goharkhah[15], as well as those of Neyestani et al. [16], are the only available works.

Microchannel heat sinks (MCHSs) featuring porous media have been proved capable ofincreasing heat transfer and decreasing pressure drop. Hence, in the present investigation, we have carried out an optimization study to determine whether a particular setup is possible that can meet both outcomes. 3D models of porous microchhannel heat sinks, including nanofluidsthat contain porous substrate walls, have been developed for this purpose.

II. PROBLEM DESCRIPTION

Fig. 1 shows the microchannel heat sink (MCHS) structure. As shown, width, height, and lengthof the MCHS are indicated by L_x, L_y, and L_z, respectively. This domain can only be modeled as a unit channel due to the periodicity of geometry. The channel is plotted in **Fig. 2**, where it has a width of w and a

height of L_v. All four solid fins have a thickness of t_s. vertical and horizontal solid fins have porous substrates with a thickness of t_p placed on each.
In the the present simulation, Ly and Lz take the values of 2.5 and 10.6 mm, respectively. Besides, we have: w=0.7 mm, ε = 0.44.

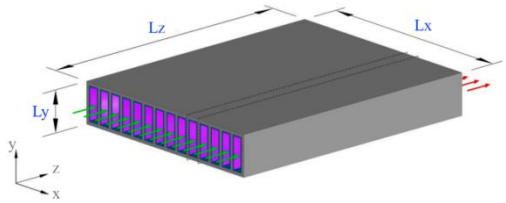


Figure 1. A schematic view of the porous MCHS geometry

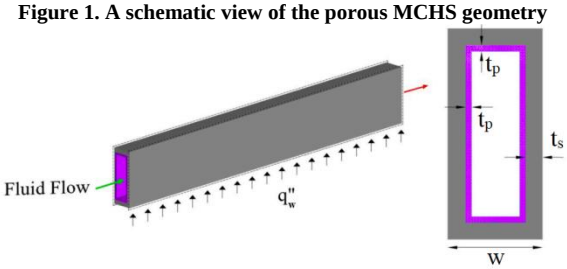


Figure 2. Microchannel heat sinks with porous substrates with geometric parameter values

2.1. Mathematical formulation

The porous-MCHS is represented by 3D designs so that coupled heat transfer can be simulated. The fluid flow is considerd laminar, incompressible and steady. There are no gravitational and radiation effects to take into account within the working temperature ranges. The thermal-physical characteristics are considered constant. An insulation condition between the heat sink and the outside environment is used. Models of fluid flow through porous domains are developed based on the equation of Forchheimer-Brinkman-Darcy derived from the volume-averaged method [17, 18]. The following equations govern continuity, momentum, and energy based on the above-mentioned assumptions [19, 20]:

$$\nabla \cdot \left(\varepsilon \rho_f \vec{V}\right) = 0 \quad (1)$$

$$\frac{\rho_f}{\varepsilon^2}(\vec{V}\cdot\nabla)\vec{V} = \nabla P - \left(\frac{\mu_f}{K_p} + \frac{\rho_f C}{\sqrt{K_p}}|\vec{V}|\right)\vec{V} + \frac{\mu_f}{\varepsilon}\nabla^2\vec{V} \quad (2)$$

$$(\rho c)_e(\vec{V}\cdot\nabla T) = k_e\nabla^2 T \quad (3)$$

where ε reresents the porous medium's porosity; ρ_f density of the fluid, $\vec{V}$ the flow's velocity, K_p permeability,P pressure, and C the Forchheimer's constant. Further, $T, \mu_f, (\rho c)_e$, and$k_e$denotetemperature, viscosity, effective heat capacity andconductivity of the porous medium, respectively. $k_e$can be calculated from $k_e = \varepsilon k_f + (1-\varepsilon)k_s$ and $(\rho c)_e$ is $(\rho c)_e = \varepsilon\rho_f c_f + (1-\varepsilon)\rho_s c_s$ in which$s$ and$f$indicate indices for solid and fluid, respectively. The equation of energy governing the solid mediumis:

$$k_s\nabla^2 T_s = 0 \quad (4)$$

where $k_s$indicatesthe solid medium's conductivity. The boundary conditions are implementedwith the following formulations:

Inlet boundary:

$$u = u_{\text{in}}, v = 0, w = 0 \text{ and } T = T_{\text{in}} \quad (5)$$

Outlet boundary:

$$P = P_0 \quad (6)$$

Solid-fluid interface:

$$\vec{V} = 0, T_f = T_s, -k_f\nabla T_f\big|_n = -k_s\nabla T_s|_n, \quad (7)$$

Here, n represents the normal unit vector on the surface.

At bottom wall:

$$q_w = -k_s\nabla T_s|_n, \quad (8)$$

At insulated walls and symmetric interfaces:

$$-k_s\nabla T_s|_n = 0 \quad (9)$$

2.2. Grid independence study

To ensure that the solution does not depend on the grids, at the beginning of the calculations, a grid independence study was performed for all geometries. In **Table 1**, an example of pressure drop calculations for a MCHS with tp = 0.1 mm is given. For this purpose, pressure drop was measured for 3 different grids, 705914, 1010705, and 1820301 for different thicknesses of solid fins. As can be seen, the results converge towards the finer grids, so that the difference between the mesh with the grid number 1010705 and 1820301 is very small. As a result, grid number 1010705 was used to continue the calculations related to this geometry.

Number of nodes	$\Delta P\ (pa)$		
	$t_s = 0.025$	$t_s = 0.06$	$t_s = 0.09$
705914	226.71	405.87	635.27
1010705	254.32	419.87	698.45
1820301	256.91	420.65	699.31

Table 1. Grid independence study

In this work, carbon nanotube (CNT)-water nanofluid flows through the microchannels. The associated thermophysical properties of water and CNT are represented in **Table 2**.

	K (W/m K)	ρ (kg/m^3)	Cp (J/kg K)
CNT	3000 [22]	3970	765 [21]
Water	0.612	998.2	4179

Table 2. Thermo-physical characteristics of the base fluid and carbon nanotube nanoparticles

The heat capacity, $(\rho C_p)_{nf}$ and the density,ρ_{nf} of the nanofluid can be calculated by:

$$(\rho C_p)_{nf} = (1-\varphi)(\rho C_p)_f + \varphi(\rho C_p)_s \quad (10)$$

$$\rho_{nf} = (1-\varphi)\rho_f + \varphi\rho_s \quad (11)$$

where volume fraction of the solid particles are denoted by φ.

III. RESULTS AND DISCUSSION

3.1. Validation

We validated our results numerically by comparing them to available numerical results. The simulation is made using microchannel hat sinks with multiple horizontal porous substrates of varying thicknesses. Comparing this simulation with that by Ghahremannezhad and Vafai[20] is given in **Table 3**. An overall good agreement between or results and those of ref. [20] can be observed.

t_s (mm)	$\bar{h}$(KWm^{-2}K^{-1})	
	Present work	Ref.[20]
0.025	7.91	7.89
0.05	9.07	8.65
0.075	10.23	9.42
0.1	10.98	10.09

Table 3. Comparison of our results with those of Ghahremannezhad and Vafai[20]

Fig. 3 illustrates the case's cross-sectional velocity and temperature fields with the conditions of t_s= 0.075 mm and t_p= 0.05 mm. Velocity has the maximum values at the center of the microchannel, and it diminishes as we move to the edges of the channel where the porous substrates are located.A bigger temperature difference can be seen at the bottom part of the vertical fin. For the temperature fields, the maximum values can be observed at the surface where the heat source $q^{"} = 100\frac{W}{cm^2}$ is implemented. Because heat is being applied to the base surface and is being transferred in a conduction manner through porous substrates, a similar pattern in temperature field should be expected.

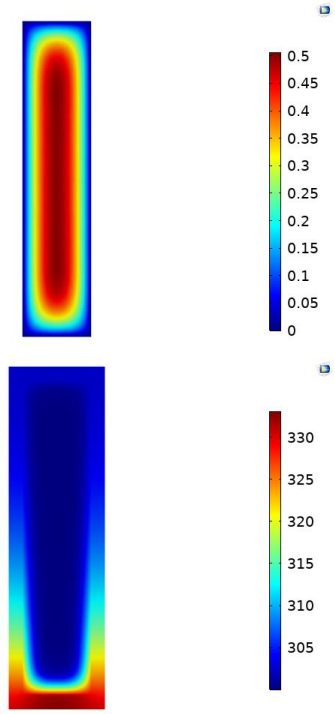


Figure 3. Velocity (left) and temperature (right) distribution at a plane located at y=5 mm for the case with ts= 0.075 mm and tp= 0.05 mm

3.2. Variations of the pressure drop with the porous thickness for different values oft_s

In this section, the functionality of the MCHS is assessed by varying the thickness of the porous substrate. The porous thickness, t_p, has changed from 0.05 mm to 0.2 mm.

The plot of the pressure drop versus thickness of the porous substrate has been shown in **Fig.4** for three thicknesses of the solid fins t_s. As can be seen, the pressure drop increases as porous thickness rises. It means that the MCHS will require more pumping power at larger porous thicknesses. It can be seen that there is no optimum point in this range of porous thickness for the pressure drop.

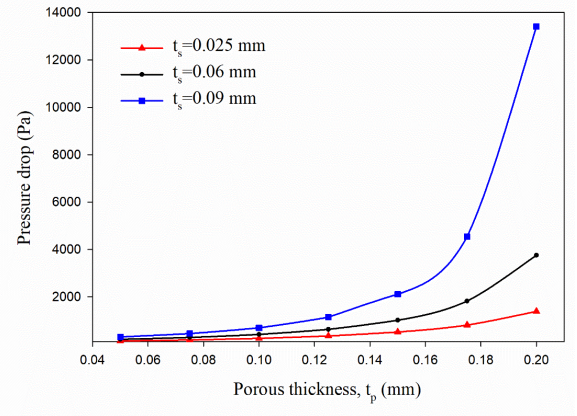


Figure 4. Changes of the pressure drop with the porous thickness

3.3. Variations of Reynolds number and heat transfer coefficient with the porous thickness for different values of t_s

The present section investigates changes of heat transfer coefficient and the dimensionless Reynolds number with the porous thickness. As can be witnessed in **Fig. 5**, as t_p increases, the Reynolds number decreases, confirming the validity of the Brinkman-Forchheimer equation. This trend is equal for all solid thicknesses (t_s). For bigger t_s, bigger Reynolds number we have. **Fig. 6** illustrates that porous substrates with higher porous thicknesses indicate higher heat transfer coefficients. The correlation between porous thickness and heat transfer coefficient is exponential for the whole solid thicknesses.

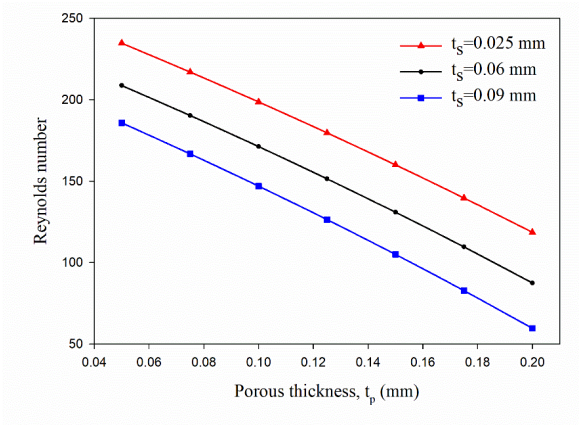


Figure 5. Variation of Reynolds number with the porous thickness

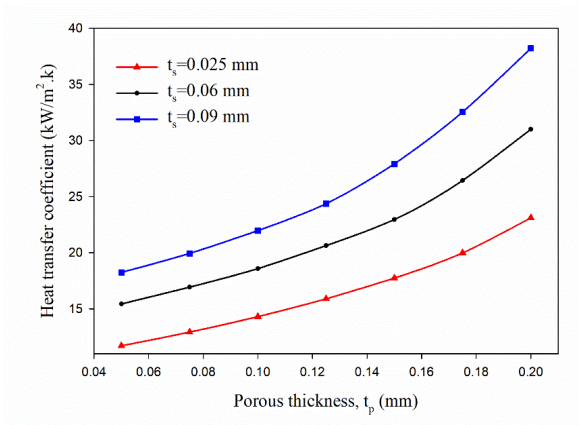


Figure 6. Changes of the h_m with the porous thickness

3.4. Changes of the pressure drop with the nanofluid volume fraction

Here, the effectiveness of the MCHS is assessed by varying the nanofluids volume fraction. The porous thickness, t_p, has varied from 0.05 mm to 0.2 mm. **Fig. 7** illustrates that as the volume fraction rises, the pressure drop augmentates, so a more powerful pump will be needed to transfer the fluid. The reason for this is the increase in the viscosity of the fluid. In the following, we will see that nanofluid leads to increased heat transfer and will be useful in this regard.

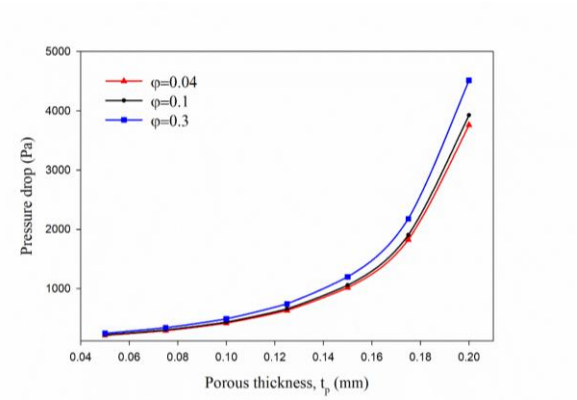


Figure 7. Variation of the pressure drop with the nanofluid volume fraction

3.5. Changes of the Reynolds number and h_m with the nanofluid volume fraction

Here, we show how the dimensionless Reynolds number and h_m change withφ. As can be seen in **Figures 8** and **9**, increasing nanofluid volume fraction leads to an augmentationin both Reynolds number and heat transfer coefficient. Because the stronger heat conductivity of the nanofluids with a higher values ofφ.

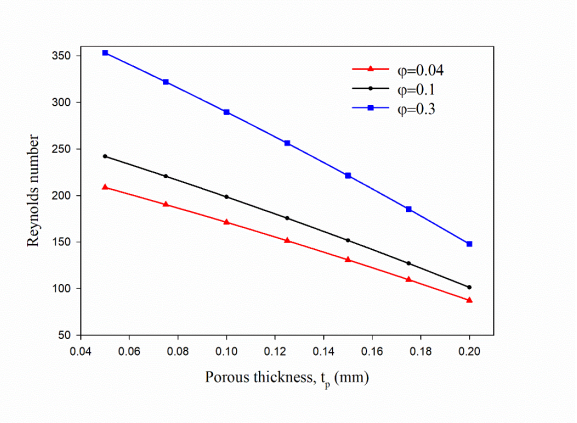


Figure 8. Changes of Reynolds number with the nanofluid volume fraction

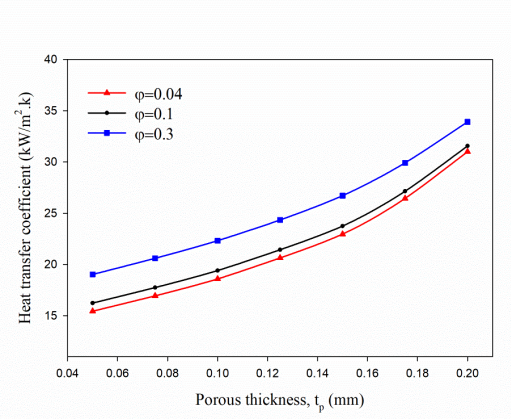


Figure 9. Changes of h_m with nanofluid volume fraction

3.6. Variation of the pressure drop with inlet velocity

Fig.10 depicts the pressure drop's change with inlet velocity. As expected, we have large pressure drops for high values of inlet velocities. Besides, the variations of pressure drop with the porous thickness differ among the three velocities of 0.2, 0.5, and 1.5 m/s. In fact the highest variations of pressure drop with porous thickness belong to the case with an inlet velocity of 1.2 m/s. As the velocity decreases, variations of pressure drop diminishes as well.

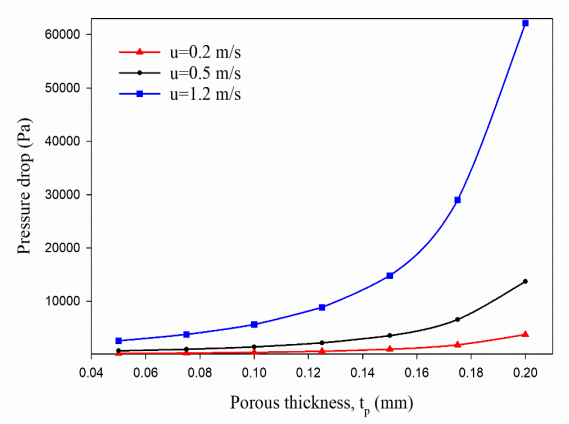


Figure 10. Changes of the pressure drop with the inlet velocity

3.7. Changes of Reynolds number and h_m with inlet velocity

Fig.11 and**Fig.12** show variations of heat transfer coefficient and Reynolds number with inlet velocity, respectively. As can be seen in **Fig. 11**, variations of Reynolds number with the porous thickness are highest for the case with an inlet velocity of **u=1.2 m/s**.When the inlet velocity is equal to u=0.2 m/s, Reynolds number change with t_p is almost negligible. Further, we have the greatest variations of h_m with tp for the case with **u=1.2 m/s,** as depicted in **Fig. 12**. It can be concluded from **Fig. 10** and **Fig. 12** that as inlet velocity increases, better heat transfer will be resulted but with the cost of a larger pressure drop.

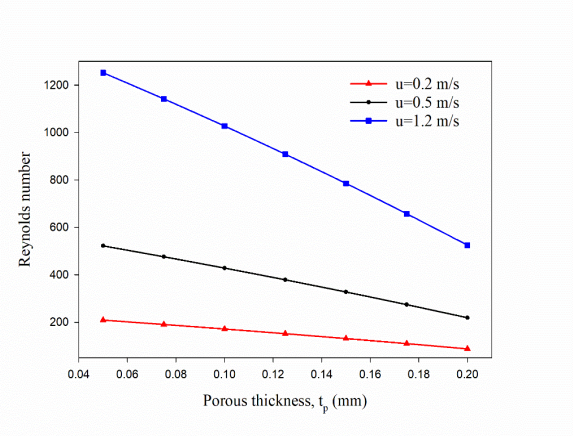


Figure 11. Variation of Reynolds number with the inlet velocity

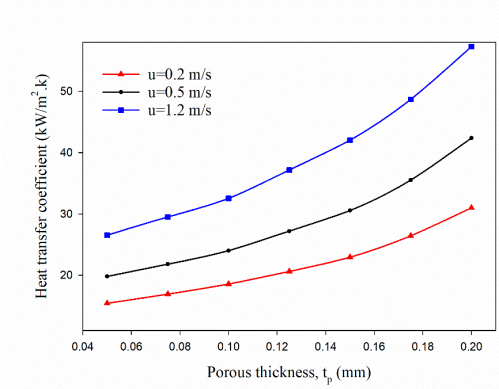


Figure 12. Variations of heat transfer coefficient with the inlet velocity

IV. CONCLUSION

In thethe present paper a porous substrate was analyzedfor optimizing the design according to pumping power thermal resistances. Our results showed that by employing a porous substrate, conventional microchannel heat sinks could be enhanced to perform better in terms of thermal performance and hydraulic efficiency. The results revealed that the pressure drop had no optimum point, and it was increased with augmentation of the porous thickness.It means that the MCHS will require more pumping power at larger porous thicknesses. The addition of a porous structure raises heat transfer for fins with a thickness in the range studied in this paper. The relationship between heat transfer coefficient and porous thickness was found to be exponential for all solid thicknesses. Further, the results revealed that increasing nanofluid volume fraction increases both Reynolds number and heat transfer coefficient. Interestingly, it was observed that the greatest variations of heat h_m and pressure drop with porous thickness are associated with the case with an inlet velocity of 1.2 m/s. As the velocity decreases, variations of the mentioned parameters diminish as well.

REFERENCES

[1] M. Adham, N. Mohd-Ghazali, and R. Ahmad, "Thermal and hydrodynamic analysis of microchannel heat sinks: A review," Renewable and Sustainable Energy Reviews, vol. 21, pp. 614-622, 2013.

[2] Y. Zhao and T. J. Lu, "Analysis of microchannel heat sinks for electronics cooling," International Journal of Heat and Mass Transfer, vol. 45, no. 24, pp. 4857-4869, 2002/11/01/ 2002, doi: https://doi.org/10.1016/S0017-9310(02)00180-1.

[3] P. Smakulski and S. Pietrowicz, "A review of the capabilities of high heat flux removal by porous materials, microchannels and spray cooling techniques," Applied Thermal Engineering, vol. 104, pp. 636-646, 2016/07/05/ 2016, doi: https://doi.org/10.1016/j.applthermaleng.2016.05.096.

[4] Agostini, M. Fabbri, J. E. Park, L. Wojtan, J. R. Thome, and B. Michel, "State of the art of high heat flux cooling technologies," Heat Transfer Engineering, vol. 28, no. 4, pp. 258-281, 2007.

[5] Weisberg, H. H. Bau, and J. N. Zemel, "Analysis of microchannels for integrated cooling," International Journal of Heat and Mass Transfer, vol. 35, no. 10, pp. 2465-2474, 1992/10/01/ 1992, doi: https://doi.org/10.1016/0017-9310(92)90089-B.

[6] G. Fedorov and R. Viskanta, "Three-dimensional conjugate heat transfer in the microchannel heat sink for electronic packaging," International Journal of Heat and Mass Transfer, vol. 43, no. 3, pp. 399-415, 2000/02/01/ 2000, doi: https://doi.org/10.1016/S0017-9310(99)00151-9.

[7] S. J. Kim and D. Kim, "Forced Convection in Microstructures for Electronic Equipment Cooling," Journal of Heat Transfer, vol. 121, no. 3, pp. 639-645, 1999, doi: 10.1115/1.2826027.

[8] W. Qu and I. Mudawar, "Analysis of three-dimensional heat transfer in micro-channel heat sinks," International Journal of Heat and Mass Transfer, vol. 45, no. 19, pp. 3973-3985, 2002/09/01/ 2002, doi: https://doi.org/10.1016/S0017-9310(02)00101-1.

[9] J. H. Ryu, D. H. Choi, and S. J. Kim, "Numerical optimization of the thermal performance of a microchannel heat sink," International Journal of Heat and Mass Transfer, vol. 45, no. 13, pp. 2823-2827, 2002/06/01/ 2002, doi: https://doi.org/10.1016/S0017-9310(02)00006-6.

[10] M. Sparrow, J. P. Abraham, and P. W. Chevalier, "A DOS-Enhanced Numerical Simulation of Heat Transfer and Fluid Flow Through an Array of Offset Fins With Conjugate Heating in the Bounding Solid," Journal of Heat Transfer, vol. 127, no. 1, pp. 27-33, 2005, doi: 10.1115/1.1800531.

[11] B. Tuckerman and R. F. W. Pease, "High-performance heat sinking for VLSI," IEEE Electron device letters, vol. 2, no. 5, pp. 126-129, 1981.

[12] Y. Alihosseini, M. Z. Targhi, M. M. Heyhat, and N. Ghorbani, "Effect of a micro heat sink geometric design on thermo-hydraulic performance: A review," Applied Thermal Engineering, vol. 170, p. 114974, 2020.

[13] S.-L. Wang, L.-Y. Chen, B.-X. Zhang, Y.-R. Yang, and X.-D. Wang, "A new design of double-layered microchannel heat sinks with wavy microchannels and porous-ribs," Journal of Thermal Analysis and Calorimetry, vol. 141, no. 1, pp. 547-558, 2020.

[14] X.-Y. Li, S.-L. Wang, X.-D. Wang, and T.-H. Wang, "Selected porous-ribs design for performance improvement in double-layered microchannel heat sinks," International Journal of Thermal Sciences, vol. 137, pp. 616-626, 2019.

[15] M. Bezaatpour and M. Goharkhah, "Effect of magnetic field on the hydrodynamic and heat transfer of magnetite ferrofluid flow in a porous fin heat sink," Journal of Magnetism and Magnetic Materials, vol. 476, pp. 506-515, 2019/04/15/ 2019, doi: https://doi.org/10.1016/j.jmmm.2019.01.028.

[16] M. Neyestani, M. Nazari, M. M. Shahmardan, M. Sharifpur, M. Ashouri, and J. P. Meyer, "Thermal characteristics of CPU cooling by using a novel porous heat sink and nanofluids," Journal of Thermal Analysis and Calorimetry, vol. 138, no. 1, pp. 805-817, 2019/10/01 2019, doi: 10.1007/s10973-019-08256-y.

[17] K. Vafai and R. Thiyagaraja, "Analysis of flow and heat transfer at the interface region of a porous medium," International Journal of Heat and Mass Transfer, vol. 30, no. 7, pp. 1391-1405, 1987/07/01/ 1987, doi: https://doi.org/10.1016/0017-9310(87)90171-2.

[18] K. Vafai, "Convective flow and heat transfer in variable-porosity media," Journal of Fluid Mechanics, vol. 147, pp. 233-259, 1984.

[19] K. Vafai and C. L. Tien, "Boundary and inertia effects on flow and heat transfer in porous media," International Journal of Heat and Mass Transfer, vol. 24, no. 2, pp. 195-203, 1981.

[20] Ghahremannezhad and K. Vafai, "Thermal and hydraulic performance enhancement of microchannel heat sinks utilizing porous substrates," International Journal of Heat and Mass Transfer, vol. 122, pp. 1313-1326, 2018.

[21] N. R. Pradhan, H. Duan, J. Liang, and G. S. Iannacchione, "The specific heat and effective thermal conductivity of composites containing single-wall and multi-wall carbon nanotubes," Nanotechnology, vol. 20, no. 24, p. 245705, 2009/05/27 2009, doi: 10.1088/0957-4484/20/24/245705.

[22] Z. Han and A. Fina, "Thermal conductivity of carbon nanotubes and their polymer nanocomposites: A review," Progress in Polymer Science, vol. 36, no. 7, pp. 914-944, 2011/07/01/ 2011, doi: https://doi.org/10.1016/j.progpolymsci.2010.11.004.

★★★